Journal of Dental Sciences 18 (2023) 310–321

Available online at www.sciencedirect.com

ScienceDirect

journal homepage: www.e-jds.com

Original Article

Anti-apoptosis and anti-inflammation activity of circ_0097010 downregulation in lipopolysaccharide-stimulated periodontal ligament cells by miR-769-5p/Krüppel like factor 6 axis

Dan-Dan Sun †, Xue Wu †, Shi-Chen Lin, Shao-Yu Duan*

Department of Stomatology, Electric Power Teaching Hospital, Capital Medical University, Beijing, China

Received 11 April 2022; Final revision received 25 April 2022
Available online 4 June 2022

KEYWORDS
Periodontitis;
Circ_0097010;
Inflammation;
MiR-769-5p;
Krüppel like factor 6 (KLF6)

Abstract *Background/purpose:* Periodontitis is a prevalent infectious inflammatory disease. Growing evidence has revealed important roles for circular RNAs (circRNAs) and circRNA sponge activity in periodontitis. Here, we elucidated the precise part of circ_0097010 in periodontitis pathogenesis.
Materials and methods: Human periodontal ligament cells (hPDLCs) were exposed to lipopolysaccharide (LPS). Cell viability, proliferation and apoptosis were evaluated by CCK-8 assay, EdU incorporation assay and flow cytometry, respectively. Circ_0097010, microRNA (miR)-769-5p and Krüppel like factor 6 (KLF6) were quantified by qRT-PCR and Western blot. Interleukin 6 (IL-6) level, tumor necrosis factor-α (TNF-α) secretion, superoxide dismutase (SOD) activity and malondialdehyde (MDA) level were detected by enzyme-linked immunosorbent assay (ELISA). Dual-luciferase reporter, RNA immunoprecipitation (RIP) and RNA pull-down assays were used to confirm the direct relationship between miR-769-5p and circ_0097010 or KLF6.
Results: Our data showed that LPS repressed cell proliferation and induced cell apoptosis and inflammation in hPDLCs. Circ_0097010 was upregulated in periodontitis samples and LPS-exposed hPDLCs. Downregulation of circ_0097010 exerted anti-apoptosis and anti-inflammation functions in LPS-exposed hPDLCs. Mechanistically, circ_0097010 acted as a miR-769-5p sponge, and reduced abundance of miR-769-5p reversed the anti-apoptosis and anti-inflammation effects of circ_0097010 suppression. KLF6 was a direct miR-769-5p target, and miR-769-5p-mediated inhibition of KLF6 possessed anti-apoptosis and anti-inflammation

* Corresponding author. Department of Stomatology, Electric Power Teaching Hospital, Capital Medical University, No.1, Taipingqiao Xili, Fengtai District, Beijing 100073, China.
E-mail address: niandentist789@163.com (S.-Y. Duan).
† Dandan Sun and Xue Wu contributed equally to this work.

https://doi.org/10.1016/j.jds.2022.04.024

functions in LPS-induced hPDLCs. Moreover, circ_0097010 controlled KLF6 expression by miR-769-5p.

Conclusion: These data identify circ_0097010 as a key regulator of LPS-induced inflammation and apoptosis in hPDLCs and highlight a novel mechanism of circ_0097010 regulation through miR-769-5p/KLF6 axis.

Introduction

As a chronic inflammatory disorder, periodontitis is a prevalent infectious disease in the tooth-supporting tissues.[1,2] Periodontitis progressively destroys all parts of the periodontium and ultimately can lead to tooth loss and other systemic diseases.[3,4] Hence, accurate diagnosis, prevention and treatment of this disease are very crucial.

Circular RNAs (circRNAs) have been recently identified as a naturally occurring family of endogenous RNA molecules with closed loops and high stability.[5] Moreover, circRNAs can absorb microRNAs (miRNAs) and serve as miRNA sponges to contribute to gene regulation.[6] Growing evidence has also revealed important roles for circRNAs and circRNA sponge activity in human diseases,[7] including periodontitis.[8,9] For example, circ_0003948 is abnormally expressed in gingival samples of patients with periodontitis and correlated with chronic periodontitis development.[10] Overexpression of circ_0081572 can protect periodontal ligament cells (PDLCs) against lipopolysaccharide (LPS)-imposed cell damage through RAR related orphan receptor A (RORA) expression regulation by sponging miR-378 h.[11] Moreover, circRNA CDR1as serves as a miR-7 sponge to impact the proliferation ability of periodontal ligament stem cells under a LPS-evoked inflammatory condition by activating the ERK signaling.[12] A previous document indicated the upregulated expression of circ_0097010 in gingival samples of periodontitis patients using Illumina sequencing.[13] Circ_0097010, generated from back-spliced exons of solute carrier family 5 member 8 (SLC5A8), is a relatively unexplored circRNA. Furthermore, no studies proved the causal role of circ_0097010 in periodontitis pathogenesis.

MiRNAs are capable of actively participating in the pathogenesis of periodontitis.[14,15] Recently, a gain-of-function study uncovers the anti-inflammation and anti-apoptosis functions of miR-769-5p in PDLCs under LPS stimulation.[16] Krüppel like factor 6 (KLF6), a member of the KLF family that can modulate crucial biological processes, has been shown to contribute to disease development upon abnormal regulation.[17] Moreover, KLF6 operates as a key regulator in periodontitis development by impacting PDLC inflammation induced by LPS.[18] Because circ_0097010 and KLF6 3'untranslated region (3′UTR) were predicted to bind to miR-769-5p via a shared complementary site using computational prediction methods, we hypothesized that circ_0097010 might contribute to KLF6 regulation through miR-769-5p competition. Herein, we used LPS-exposed human PDLCs (hPDLCs) to preliminarily elucidate the precise part played by circ_0097010 in periodontitis pathogenesis.

Materials and methods

Cell culture and treatment

In this work, we used primary fibroblastic hPDLCs (ScienCell Research Laboratories, Carlsbad, CA, USA) at passages lower than 7. We propagated hPDLCs using α-Minimum Essential Medium (α-MEM, Wako, Saitama, Japan) containing 10% FBS (Biowest, Nuaillé, UK) and 1% streptomycin/penicillin (Leagene, Beijing, China) at 5% CO_2 at 37 °C.

We procured LPS (*Escherichia coli* 055:B5, ≥99% purity) from Solarbio (Beijing, China). For LPS stimulation, hPDLCs were grown at 5×10^5 cells per 100-mm dish and exposed to LPS at a 2 μg/mL concentration for 24 h. For the dose course experiment of LPS exposure, hPDLCs were incubated for 24 h with LPS at a concentration of 0, 1, 2, or 4 μg/mL and then subjected afterward to cell viability analysis.

siRNA oligos, miRNA mimics, miRNA inhibitors and plasmids and transient transfection of hPDLCs

siRNA for circ_0097010 (si-circ_0097010, 5′-GGAUUAAAACUGCAACAAAGC-3′) was designed using circInteractome online tool (https://circinteractome.nia.nih.gov/index.html) based on the junction sequence and synthesized by Geneseed (Guangzhou, China). As the control, a nontarget siRNA oligo (si-NC, 5′-GCAAUUAUAGUCCUAGAUACC-3′, Geneseed) was used. Silencer® KLF6 siRNA (si-KLF6) and negative control #2 siRNA (si-con) were procured from Thermo Fisher Scientific (Milan, Italy). MicrON miR-769-5p mimic and inhibitor (anti-miR-769-5p) were procured from Ribobio (Guangzhou, China). Negative mimic and inhibitor controls (miR-NC and anti-miR-NC, Ribobio) have been verified to have minimal sequence identity with miRNAs in humans. The PCR-amplified KLF6 coding sequence (without 3′UTR) was digested with BamH I and Xho I and then inserted into the same sites of the pcDNA3.1 (+) vector (YouBio, Changsha, China) to produce KLF6 expression plasmid, and a nontarget pcDNA vector served as the control. pCD5-ciR-based circ_0097010 expression plasmid and control plasmid pCD5-ciR were procured from Geneseed.

hPDLCs (5×10^3 cells/well) were plated in the wells of a 96-multiwell dish one day before transfection using Superfect (Qiagen, Hombrechtikon, Switzerland) and then each well was afterward introduced with 10 nM siRNA or/and

20 ng plasmid or/and 5 nM miRNA mimic/inhibitor oligo as per the manufacturing guideline. Transfection was allowed for 6 h at 37 °C and cells were then incubated at 37 °C for 24 h before LPS exposure.

CCK-8 cell viability assay

We performed a CCK-8 (cell counting Kit-8) assay to analyze cell viability after the indicated transfection or/and LPS exposure as above. 10% CCK-8 solution (Genomeditech, Shanghai, China) in media was added before incubating for 3 h at 37 °C. We gauged the absorption at 450 nm by spectrophotometry (Infinite 200Pro, Tecan, Mannedorf, Switzerland).

EdU cell proliferation assay

We employed the EdU (5-ethynyl-2′-deoxyuridine) incorporation assay to evaluate cell proliferation. After hPDLCs were processed by the indicated transfection or/and LPS exposure as above, 50 μM EdU solution (Invitrogen, Hemel Hempstead, UK) in media was added before incubating at 37 °C for 2 h, followed by the consecutive staining with 1 × Apollo®567 (Ribobio) and DAPI (4′,6-diamidino-2-phenylindole, Roche, Vilvoorde, Belgium). Under fluorescence microscopy (Leica, Bensheim, Germany), we determined the ratio of the EdU positive cells/total nuclei.

Cell apoptosis by flow cytometry

For cell flow cytometry, after the indicated transfection or/and LPS exposure, hPDLCs were subjected to Annexin V-FITC (Roche, 25 μg/mL) and propidium iodide (PI, Invitrogen, 50 μg/mL) staining as recommended by the manufacturers. Using an LSRII cytometer (BD Biosciences, Heidelberg, Germany) and FlowJo 9.1 software (TreeStar, Ashland, OR, USA), we analyzed stained cells and defined apoptotic cells that were positive for Annexin V.

Western blot

We performed immunoblotting using total protein samples extracted with RIPA buffer containing protease inhibitors as described.[19] Protein extracts were resolved by electrophoresis for separation and then transferred onto nitrocellulose membranes (Merck Millipore, Darmstadt, Germany). Protein detection was conducted using the following primary antibodies: rabbit polyclonal anti-KLF6 (Cat#PA5-79560, dilution 1:500, Invitrogen), rabbit polyclonal anti-Bax (Cat#abc11, dilution 1:500, Merck Millipore), mouse monoclonal anti-Bcl-2 (Cat#MA5-11757, dilution 1:50, Invitrogen), and mouse monoclonal anti-GAPDH (Cat#ab8245, dilution 1:3,000, Abcam, Cambridge, UK). We used the Image Lab software (Bio-Rad, Gladesville, NSW, Australia) for densitometric analysis after addition of a chemiluminescent substrate (Merck Millipore).

Enzyme-linked immunosorbent assay (ELISA)

The Human Interleukin 6 (IL-6) ELISA Kit (Invitrogen) and Human Tumor Necrosis Factor-α (TNF-α) ELISA Kit (Boster, Wuhan, China) were applied to evaluate the secretion levels of IL-6 and TNF-α in culture medium, respectively, as per the accompanying suggestion. The superoxide dismutase (SOD) activity and malondialdehyde (MDA) level in hPDLCs after the indicated transfection or/and LPS exposure were gauged by the SOD Activity Colorimetric Assay Kit (Abcam) and MDA Colorimetric Assay Kit (Elabsience, Wuhan, China), respectively, based on the manufacturers' recommendations.

Human gingival specimens

We harvested human gingival tissue specimens from patients with periodontitis (n = 22; 4 cases of mild, 7 cases of moderate, 11 cases of severe) and sex- and age-matched healthy donors (teeth for orthodontic, n = 19) who gave informed consent at Electric Power Teaching Hospital, Capital Medical University. The median age of the patients (12 females and 10 males) was 33.6 years (with a range of 27—52 years). The median age of the donors (10 females and 9 males) was 31.4 years (with a range of 23—57). Patients with other oral or systemic diseases were excluded from this study. These specimens were kept at −80 °C until required. Human study obtained the ratification of the Ethics Committee of Electric Power Teaching Hospital, Capital Medical University.

RNA extraction, RNase R treatment and RNA expression analysis by qRT-PCR

The Aurum™ Total RNA Mini Kit (Bio-Rad) was utilized for RNA extraction from hPDLCs and human specimens. For RNase R digestion experiment, 0 or 3 U RNase R (Geneseed) was added to 1 μg RNA from hPDLCs, followed by heating to 37 °C for 15 min. For circ_0097010, KLF6 mRNA and GAPDH (a reference gene) mRNA analyses, RNA (1 μg) was converted into cDNA using RT^2 First Strand Kit (Qiagen) and further amplified following iQ SYBR Green (Bio-Rad) protocols. For miR-769-5p and U6 (a housekeeping gene) analyses, we employed the miScript miRNA qRT-PCR assays (Qiagen) as described by the manufacturers. Using the $2^{-\Delta\Delta Ct}$ method, we determined the fold change, following normalisation to GAPDH or U6 expression. Primer sequences were listed in Supplement Table 1.

Computational prediction

For prediction of miRNA-binding sites to circ_0097010, we interrogated the online bioinformatics programs circInteractome and circBank (http://www.circbank.cn/). For prediction of miR-769-5p target genes, we utilized the targetScan prediction program (http://www.targetscan.org/vert_72/).

Dual-luciferase reporter assay

We procured the synthesized fragments of circ_0097010 and KLF6 3′UTR encompassing the miR-769-5p target region or miss-matched seed sequence from Comate Bioscience (Changchun, China). Reporter constructs were generated by inserting the synthesized sequence into the 3′UTR of *Renilla* luciferase on a psiCHECK-2 vector (Promega, Vienna, Austria). hPDLCs (5×10^5 cells/well) grown in a 12-multiwell dish were introduced using Superfect reagent with 200 ng reporter vector and 30 nM miRNA mimic. Using the Dual-luciferase Assay System (Promega), we calculated the ratio of *Renilla* luciferase to firefly luciferase for each well.

RNA immunoprecipitation (RIP) and RNA pull-down assays

Whole cell lysates were acquired following RIPA buffer protocols. For RIP experiment, we incubated (6 h; 4 °C) cell lysates with Protein A/G Agarose (Yeasen, Shanghai, China) previously coupled with rabbit monoclonal anti-Ago2 (Cat#ab233727, dilution 1:100, Abcam) or anti-IgG (Cat#ab172730, dilution 1:300, Abcam) antibody. For RNA pull-down experiment, we incubated (6 h; 4 °C) cell lysates with streptavidin magnetic beads (Roche) previously coupled with a biotinylated miR-769-5p mimic probe (bio-miR-769-5p) and control Oligo probe (bio-miR-NC, both from Viagene, Changzhou, China). RNA bound to beads was used for qRT-PCR to gauge the levels of circ_0097010, miR-769-5p and KLF6.

Statistical analysis

All data were representative of at least three independent experiments and presented as the mean and SEM. Differences were considered significant at values of $P < 0.05$ by ANOVA with *post hoc* Tukey's multiple comparisons test (three or more groups) or Student's *t*-test (two groups). Expression correlation analyses were done using Pearson's correlation coefficient.

Results

Circ_0097010 is overexpressed in periodontitis samples and suppression of circ_0097010 exerts anti-apoptosis and anti-inflammation functions in LPS-induced hPDLCs

We firstly confirmed the cytotoxic impact of LPS on hPDLCs. In hPDLCs, LPS exposure led to a marked inhibition in cell viability and proliferation (Fig. 1A and B) and increased cell apoptosis (Fig. 1C and D) compared with the control group. The pro-apoptosis activity of LPS was also validated by detection of the expression of pro-apoptotic protein Bax and anti-apoptotic factor Bcl-2. LPS-induced hPDLCs exhibited higher levels of Bax and lower expression of Bcl-2 than controls (Fig. 1E). LPS exposure also resulted in a significant elevation in pro-inflammatory cytokines (IL-6 and TNF-α) expression (Fig. 1F and G). Additionally, LPS clearly inhibited SOD activity and enhanced MDA production in hPDLCs (Fig. 1H and I). All these results confirm that LPS impairs cell proliferation and induces cell apoptosis and inflammation in hPDLCs.

To determine if circ_0097010 is relevant in periodontitis pathogenesis, we tested by qRT-PCR for circ_0097010 expression in gingival tissue samples of patients with periodontitis. Relative to normal tissue samples, circ_0097010 was remarkably upregulated in periodontitis samples (Fig. 2A). Moreover, with the increase of the severity of gingivitis in subjects, circ_0097010 expression was progressively upregulated (Fig. 2A). The RNase R resistance of circ_0097010 was also ascertained by RNase R digestion experiments (Fig. 2B). Through qRT-PCR, we also found that LPS induced circ_0097010 expression in hPDLCs (Fig. 2C). To examine the relevance of circ_0097010 expression in LPS-induced injury in hPDLCs, we counteracted circ_0097010 upregulation induced by LPS using a siRNA specific for circ_0097010 (si-circ_0097010). The circ_0097010 downregulation efficacy of si-circ_0097010 introduction was confirmed by qRT-PCR (Fig. 2C). In contrast, suppression of circ_0097010 rescued LPS-imposed viability and proliferation defects (Fig. 2D and E) and abated cell apoptosis induced by LPS (Fig. 2F and G) in hPDLCs. Furthermore, suppression of circ_0097010 abolished the impact of LPS on IL-6 production (Fig. 2H), TNF-α secretion (Fig. 2I), SOD activity (Fig. 2J) and MDA expression (Fig. 2K) in hPDLCs. Additionally, elevated expression of circ_0097010 upon the expression plasmid transfection, validated by qRT-PCR, significantly exacerbated LPS-imposed viability and proliferation defects, apoptosis enhancement, and inflammation increase in hPDLCs (Supplement Fig. 1A–1F). Overexpression of circ_0097010 also diminished SOD activity and increased MDA level in LPS-stimulated hPDLCs (Supplement Fig. 1G and 1H). These results indicate that downregulation of circ_0097010 relieves hPDLC apoptosis and inflammation induced by LPS.

Circ_0097010 acts as a sponge of miR-769-5p

To determine if circ_0097010 can function as miRNA sponges, we decided to utilize the online bioinformatics programs circInteractome and circBank. Interestingly, a putative miR-769-5p complementary region in circ_0097010 was predicted by both the two programs (Fig. 3A). To confirm this, the circ_0097010 fragment containing the target region was cloned into the psiCHECK-2 luciferase plasmid downstream of the *Renilla* luciferase open reading frame. This reporter construct was used to transfect hPDLCs along with miR-769-5p mimic. Elevated expression of miR-769-5p upon transfection, validated by qRT-PCR (Fig. 3B), markedly diminished luciferase expression of this construct (Fig. 3C). We subsequently generated mutations in the target region. When we performed luciferase assays using a plasmid harboring the mutated target region, we observed no reduction in luciferase with miR-769-5p overexpression (Fig. 3C). Ago2 is the core component of the RNA-induced silencing complexes (RISCs), where miRNAs post-transcriptionally silence gene expression.[20] We thus performed RIP experiments using an antibody specific for Ago2 on extracts of hPDLCs. Circ_0097010 and miR-769-

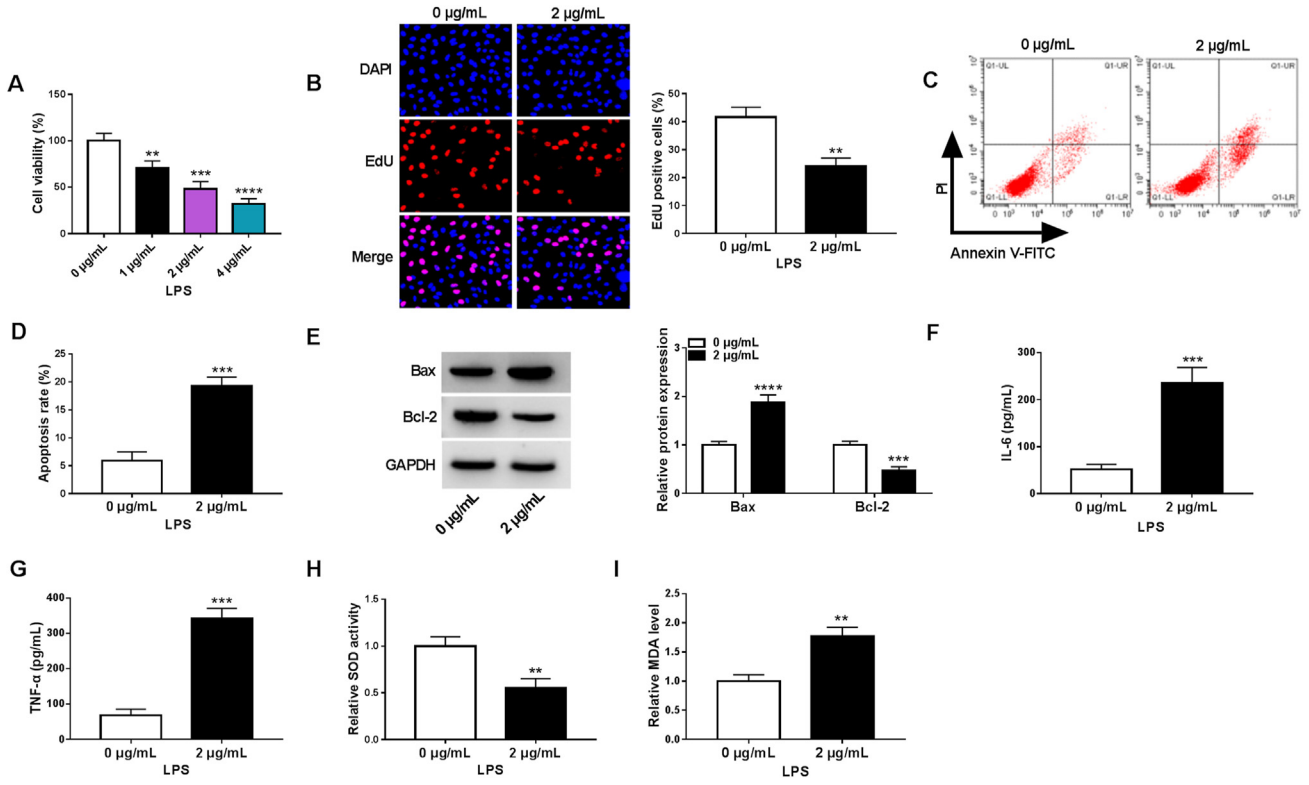

Figure 1 LPS impairs cell proliferation and induces apoptosis and inflammation in hPDLCs. (A) CCK-8 cell viability assay with hPDLCs after stimulation with the indicated doses of LPS for 24 h. (B—I) EdU cell proliferation assay (B), flow cytometry for cell apoptosis (C and D), Bax and Bcl-2 expression levels by Western blot (E), the production levels of IL-6 and TNF-α by ELISA using the assay kits (F and G), SOD activity and MDA level using the assay kits (H and I) in hPDLCs exposed to 0 or 2 μg/mL of LPS for 24 h. $^{**}P < 0.01$, $^{***}P < 0.001$, $^{****}P < 0.0001$.

5p were strongly enriched in Ago2-containing RISCs compared with IgG control immunoprecipitates (Fig. 3D), suggesting the association between circ_0097010 and the RISCs. Through RNA pull-down assays using biotinylated miR-769-5p mimic (bio-miR-769-5p), we ascertained the direct relationship between circ_0097010 and miR-769-5p (Fig. 3E). Analysis of miR-769-5p expression by qRT-PCR showed the underexpression of miR-769-5p in periodontitis samples relative to normal controls (Fig. 3F). With the increase of the severity of gingivitis in subjects, miR-769-5p expression was progressively reduced (Fig. 3F). Using nonparametric test analysis, we found a significant inverse correlation between miR-769-5p expression and circ_0097010 level in periodontitis samples ($r = -0.8083$, $p < 0.001$) (Fig. 3G). Furthermore, in hPDLCs, LPS led to a clear downregulation in miR-769-5p expression (Fig. 3H). Hence, circ_0097010 acts as a miR-769-5p sponge in hPLDCs.

Decreased abundance of miR-769-5p reverses the anti-apoptosis and anti-inflammation functions of circ_0097010 suppression in LPS-induced hPDLCs

In LPS-induced hPDLCs, we observed that downregulation of circ_00769-5p resulted in increased abundance of available miR-769-5p (Fig. 4A). We then wanted to test whether circ_0097010's ability to impact cell inflammation and apoptosis in LPS-induced hPDLCs is due to its role as a miR-769-5p sponge. To resolve this, an inhibitor of miR-769-5p (anti-miR-769-5p) was used to co-transfect hPDLCs with si-circ_0097010 before LPS exposure. Through qRT-PCR, co-transfection of anti-miR-769-5p abated si-circ_0097010-imposed miR-769-5p expression elevation in LPS-exposed hPDLCs (Fig. 4A). Notably, decrease of miR-769-5p diminished cell viability and proliferation induced by circ_0097010 downregulation in LPS-treated hPDLCs (Fig. 4B and C). Meanwhile, miR-769-5p decrease abolished circ_0097010 downregulation-mediated repression of apoptosis and pro-inflammatory cytokine (IL-6 and TNF-α) expression of LPS-induced hPDLCs (Fig. 4D—H). Additionally, miR-769-5p decrease abolished the impact of si-circ_0097010 on SOD activity and MDA level in hPDLCs under LPS (Fig. 4I and J). All these data suggest that suppression of circ_0097010 exerts anti-apoptosis and anti-inflammation functions in LPS-induced hPDLCs at least partially by increasing miR-679-5p abundance.

KLF6 is a direct miR-769-5p target and circ_0097010 regulates KLF6 expression by miR-769-5p

To establish miR-769-5p effectors, we interrogated the targetScan prediction program. Of interest, the predicted data revealed that the sequence of miR-769-5p aligned with

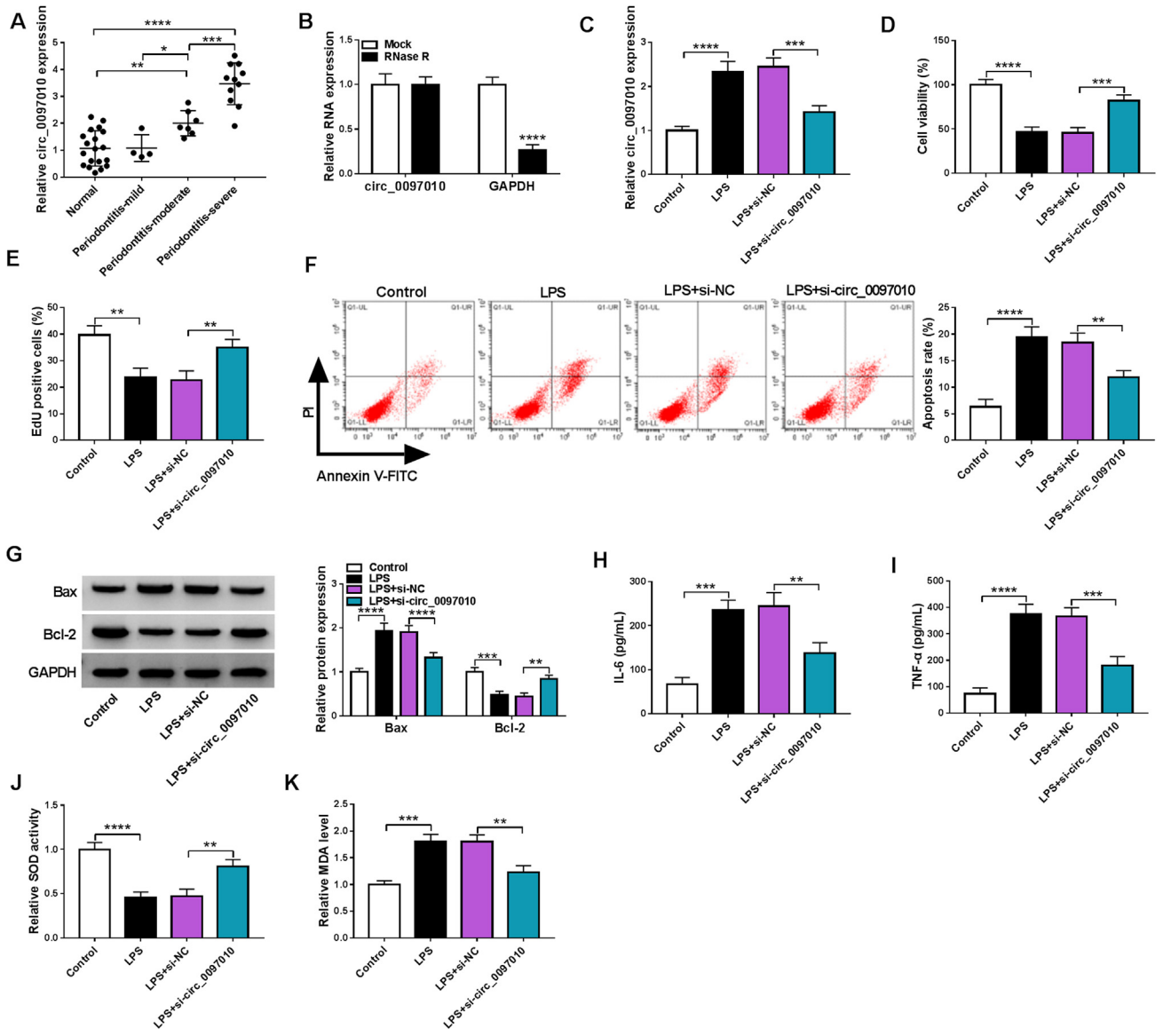

Figure 2 Downregulation of circ_0097010 mitigates LPS-driven anti-proliferation, pro-apoptosis and pro-inflammation effects on hPDLCs. (A) Relative circ_0097010 expression by qRT-PCR in gingival tissue samples of patients with periodontitis (n = 22) and healthy volunteers (n = 19). (B) Effect of RNase R digestion on the levels of circ_0079010 and GAPDH. (C–K) hPDLCs were transiently introduced with or without si-circ_0079010 or si-NC before stimulation with 0 or 2 μg/mL of LPS for 24 h. (C) qRT-PCR of relative circ_0079010 expression in hPDLCs after treatment as indicated. (D) CCK-8 cell viability assay with hPDLCs treated as indicated. (E) Assessment of cell proliferation by EdU assay after the indicated treatment. (F) Detection of cell apoptosis by flow cytometry based on the staining with Annexin V and PI. (G) Western blot of Bax and Bcl-2 levels in hPDLCs after the indicated treatment. (H and I) The production levels of IL-6 and TNF-α in treated hPDLCs by ELISA using the assay kits. (J and K) SOD activity and MDA level in treated hPDLCs using the assay kits. $^{**}P < 0.01$, $^{***}P < 0.001$, $^{****}P < 0.0001$.

nucleotides in the KLF6 3′UTR (Fig. 5A). We confirmed that KLF6 is a direct target of miR-769-5p, using a luciferase reporter linked to the KLF6 3′UTR (Fig. 5B): co-transfection of this construct (WT) with miR-769-5p mimic into hPDLCs resulted in a striking reduction in luciferase activity; site-directed mutation (MUT) of the miR-769-5p pairing sequence in the KLF6 3′UTR completely abolished it effect (Fig. 5B). Furthermore, the results of RIP and RNA pull-down experiments reinforced the targeting of KLF6 by miR-769-5p (Fig. 5C and D). We also examined periodontitis samples and normal controls and validated a significant overexpression of KLF6 mRNA in periodontitis samples relative to normal controls (Fig. 5E). Intriguingly, KLF6 mRNA expression was progressively elevated with the increase of the severity of gingivitis in subjects (Fig. 5E). Correlation analysis between KLF6 mRNA expression and miR-769-5p showed a striking inverse correlation (Fig. 5F). Western blot data also revealed the upregulation of KLF6 protein in periodontitis samples and LPS-induced hPDLCs (Fig. 5G and H).

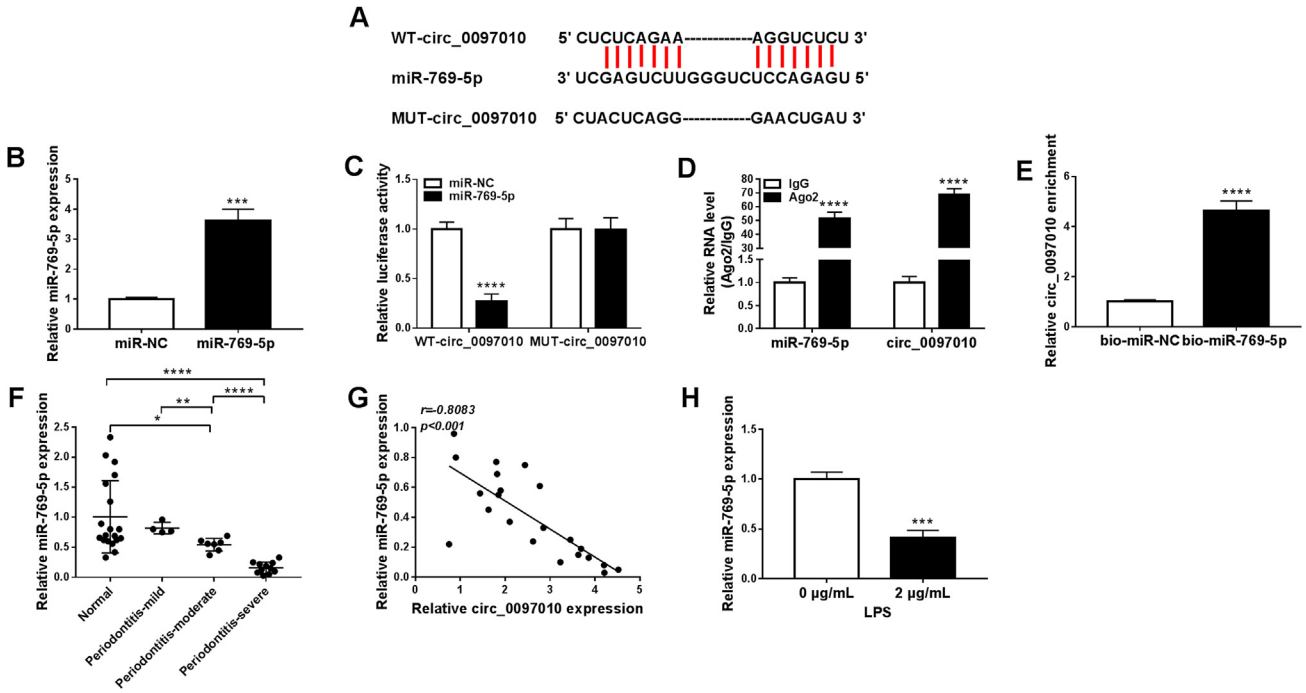

Figure 3 Circ_0097010 sponges miR-769-5p. (A) Sequence of miR-769-5p, the potential miR-769-5p complementary sites at circ_0097010, and the mutated target sequence in circ_0097010. (B) qRT-PCR showing the transfection efficiency of miR-769-5p mimic. (C) Luciferase activity of the wild-type (WT) or mutant (MUT) reporter constructs after transfection with miR-769-5p mimic or miR-NC mimic. (D) RIP experiments on extracts of hPDLCs using an antibody against Ago2 or IgG. (E) RNA pull-down assays on extracts of hPDLCs using bio-miR-769-5p or bio-miR-NC. (F) Relative miR-769-5p expression by qRT-PCR in gingival tissue samples of patients with periodontitis (n = 22) and healthy volunteers (n = 19). (G) Expression correlation analysis of miR-769-5p and circ_0079010 in periodontitis samples (n = 22) using Pearson's correlation coefficient. (H) qRT-PCR of miR-769-5p in hPDLCs after exposure to 0 or 2 μg/mL of LPS for 24 h. ***$P < 0.001$, ****$P < 0.0001$.

Given the shared binding site of circ_0097010 and KLF6 3′UTR in miR-769-5p, we hypothesized that circ_0097010 might interfere with KLF6 expression by sponging miR-769-5p. KLF6 protein expression was also remarkably reduced in LPS-induced hPDLCs after transfection by si-circ_0097010, and this effect was counteracted by decreased miR-769-5p expression (Fig. 5I). We therefore conclude that circ_0097010 sponges miR-769-5p to control KLF6 expression.

MiR-769-5p-mediated inhibition of KLF6 exerts anti-apoptosis and anti-inflammation functions in LPS-induced hPDLCs

In LPS-induced hPDLCs, elevated expression of miR-769-5p upon transfection led to a marked reduction in KLF6 protein expression (Fig. 6A), increased cell viability and proliferation (Fig. 6B and C), suppressed cell apoptosis (Fig. 6D—F), and caused a significant downregulation of IL-6 and TNF-α production levels (Fig. 6G and H). Meanwhile, miR-769-5p upregulation increased SOD activity and diminished MDA expression level in hPDLCs under LPS exposure (Fig. 6I and J).

Additionally, downregulation of KLF6 protein by si-KLF6 transfection promoted cell viability and proliferation and impeded cell apoptosis, as well as diminished the production levels of IL-6 and TNF-α in LPS-induced hPDLCs (Supplement Fig. 2A—2H). Downregulation of KLF6 also enhanced SOD activity and weakened MDA level in hPDLCs under LPS (Supplement Fig. 2I and 2J).

To determine if inhibition of KLF6 protein by miR-769-5p might provide an exploration for cell alterations observed following miR-769-5p, we performed a rescue experiment in miR-769-5p-overexpressing cells by expressing KLF6 protein with a plasmid construct that encodes KLF6 coding sequence without the 3′UTR. Restoration of KLF6 protein upon transfection, confirmed by Western blot (Fig. 6A), remarkably abrogated miR-769-5p-mediated pro-viability, pro-proliferation (Fig. 6B and C), anti-apoptosis (Fig. 6D—F), and anti-inflammation (Fig. 6G and H) effects in hPDLCs under LPS. KLF6 restoration also counteracted the alterations of SOD activity and MDA level following miR-769-5p upregulation in LPS-induced hPDLCs (Fig. 6I and J). These findings collectively demonstrate that KLF6 is an important effector of miR-769-5p.

Discussion

CircRNAs can operate as miRNA sponges to mediate gene regulation post-transcriptionally that have emerged as essential modulators in human diseases, including periodontitis.[8,9,21] In the current work, we focused on circ_0097010 due to its overexpression in gingival samples of periodontitis patients.[13] Our results also validate the

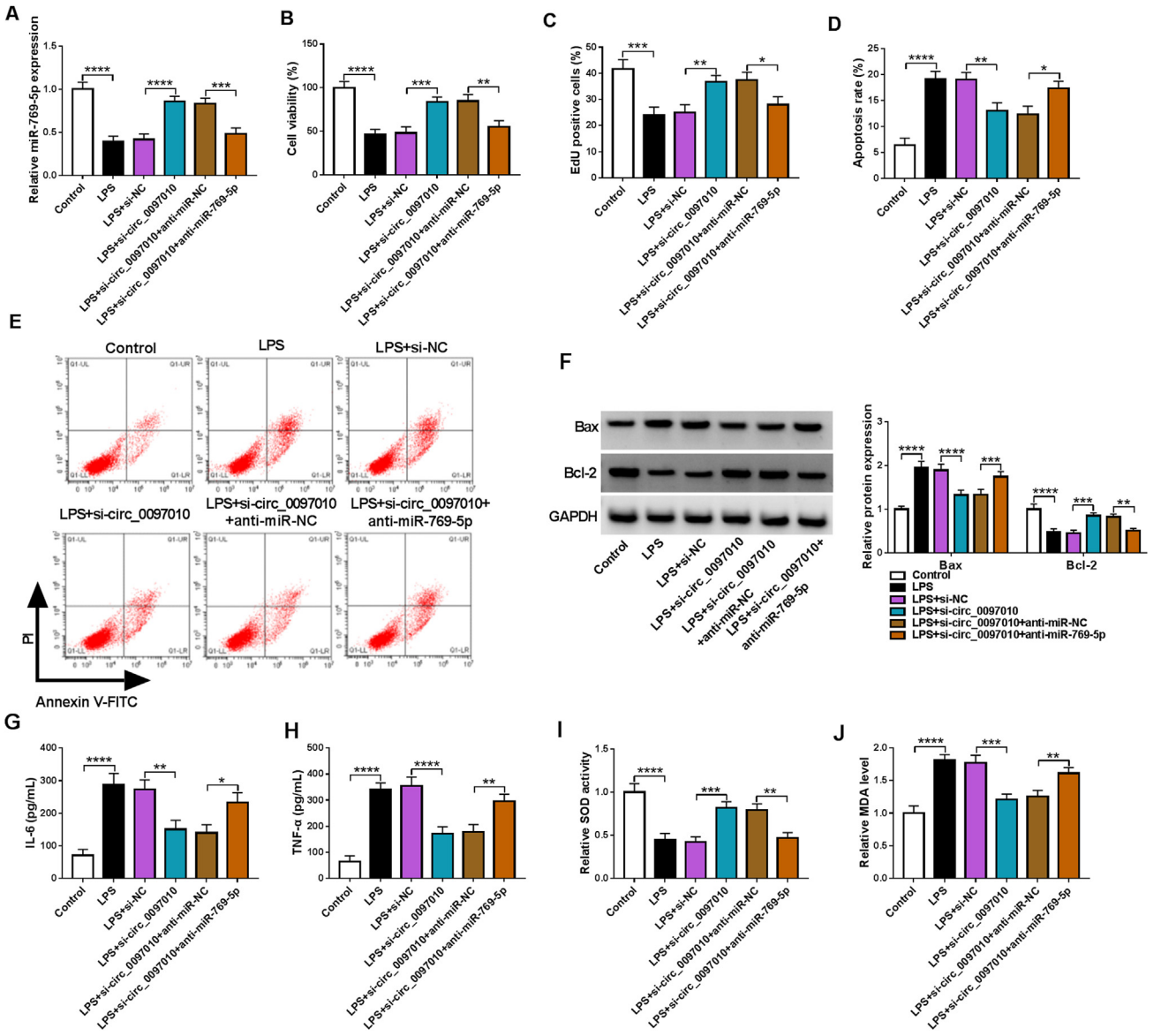

Figure 4 Decrease of miR-769-5p reverses circ_0097010 suppression-mediated anti-apoptosis and anti-inflammation functions in LPS-exposed hPDLCs. (A–J) hPDLCs were exposed to 0 or 2 μg/mL of LPS for 24 h after transfection with or without anti-miR-769-5p + si-circ_0097010, anti-miR-NC + si-circ_0097010, si-circ_0097010 or si-NC. (A) Relative miR-769-5p expression by qRT-PCR in treated hPDLCs. (B) CCK-8 cell viability assay with hPDLCs after the indicated transfection. (C) EdU cell proliferation assay with treated hPDLCs. (D and E) Cell apoptosis measurement by flow cytometry using staining with Annexin V and PI. (F) Western blot of the levels of Bax and Bcl-2 in hPDLCs after the indicated transfection. (G and H) ELISA of IL-6 and TNF-α levels in treated hPDLCs using the assay kits. (I and J) SOD activity and MDA level in treated hPDLCs using the assay kits. *$P < 0.05$, **$P < 0.01$, ***$P < 0.001$, ****$P < 0.0001$.

upregulation of circ_0097010 in LPS-exposed hPDLCs. As previously reported,[11,22] LPS induces cell apoptosis and inflammatory injury in hPDLCs. According to our siRNA silencing experiments, suppression of circ_0097010 in LPS-exposed hPDLCs exerts anti-apoptosis and anti-inflammation functions. Furthermore, we have established a novel regulatory mechanism mediated by circ_0097010 in LPS-evoked cell damage in hPDLCs. In addition, in agreement with other circRNAs,[23,24] circ_0097010 is resistant to exoribonuclease RNase R due to no free 5′ and 3’ ends in its structure.

Functional studies in cancer pathogenesis suggest that miR-769-5p has contradictory effects on human tumorigenesis. For instance, miR-769-5p is a well-established oncogene in prostate cancer, osteosarcoma and gastric cancer.[25–27] On the other hand, miR-769-5p hinders tumor development in oral squamous cell carcinoma and non-small cell lung cancer.[28,29] Moreover, circulating miR-769-5p in plasma may be a potential biomarker for mycobacterium tuberculosis infection.[30] In this work, we first demonstrate that circ_0097010 sponges miR-769-5p. Consistent with a recent document,[16] our results

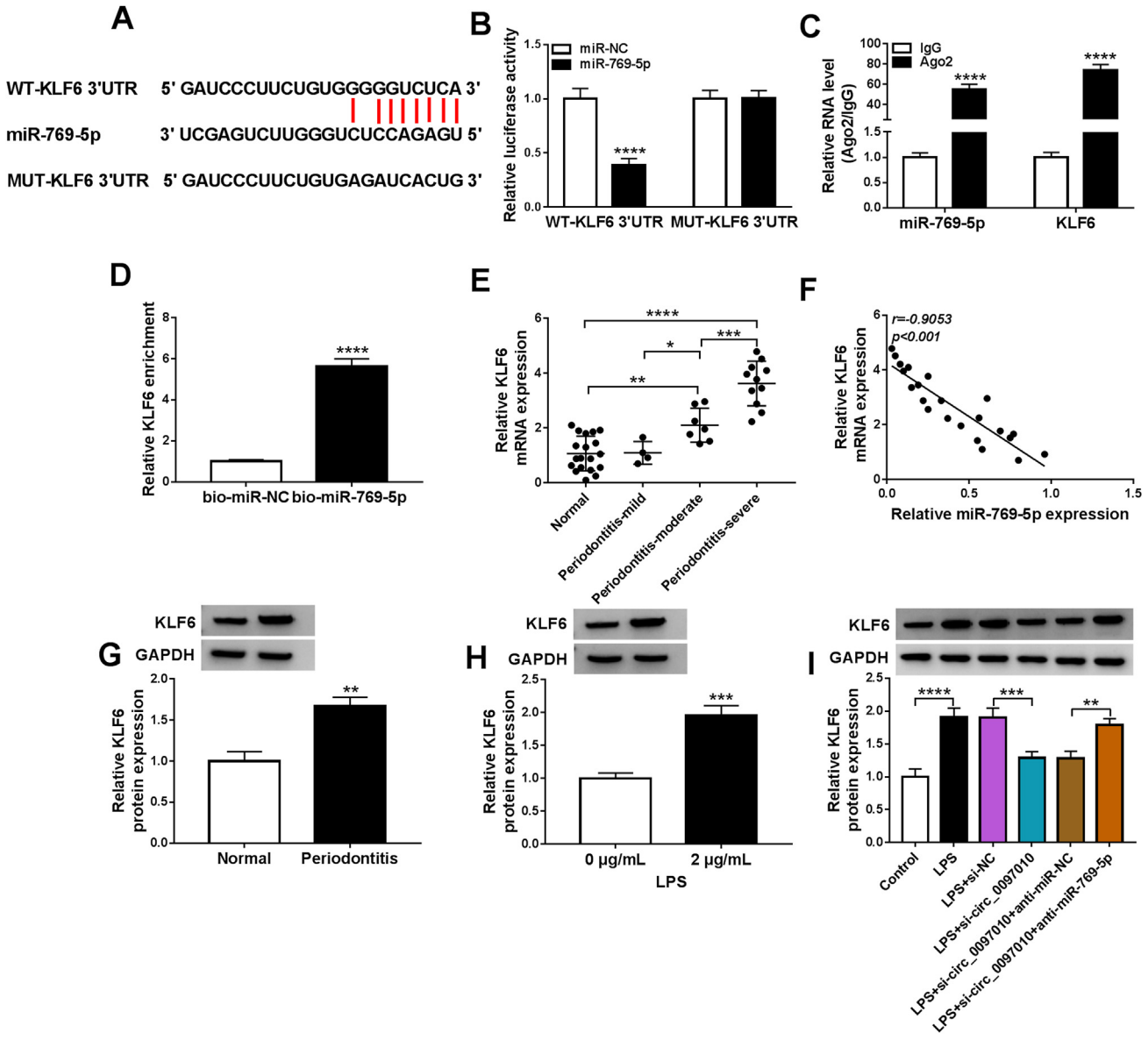

Figure 5 KLF6 is a direct miR-769-5p target and circ_0097010 controls KLF6 expression by miR-769-5p. (A) Alignment between miR-769-5p and the 3′UTR of human KLF6 and the mutations in the target sequence. (B) Luciferase activity of the wild-type (WT) or mutant (MUT) KLF6 3′UTR reporter constructs transfected into hPDLCs in the presence of miR-796-5p mimic or mimic control. (C) RIP experiments on extracts of hPDLCs using an antibody against Ago2 or IgG. (D) RNA pull-down assays on extracts of hPDLCs using bio-miR-769-5p or bio-miR-NC. (E) Quantification of KLF6 mRNA expression by qRT-PCR in gingival tissue samples of patients with periodontitis (n = 22) and healthy volunteers (n = 19). (F) Correlation analysis between KLF6 mRNA and miR-769-5p expression in periodontitis samples (n = 22) using Pearson's correlation coefficient. (G) Western blot of KLF6 protein in gingival tissue samples of patients with periodontitis (n = 3) and healthy volunteers (n = 3). (H) KLF6 protein expression by Western blot of lysates from hPDLCs after exposure to 0 or 2 μg/mL of LPS for 24 h. (I) Representative Western blot showing KLF6 protein level in LPS-treated hPDLCs after transfection by anti-miR-769-5p + si-circ_0097010, anti-miR-NC + si-circ_0097010, si-circ_0097010 or si-NC. $^{**}P < 0.01$, $^{***}P < 0.001$, $^{****}P < 0.0001$.

illuminate the anti-inflammation and anti-apoptosis functions of miR-769-5p in LPS-exposed hPDLCs. Intriguingly, we point to, for the first time, miR-769-5p as a functional mediator of circ_0097010 in impacting LPS-evoked hPDLC inflammation and apoptosis.

Deregulated KLF6 activity can induce the development of cancer, cardiovascular diseases and inflammatory diseases.[17] KLF6 has established a promoting role in cell inflammation by working as the mediator of pro-inflammatory response.[31–33] Furthermore, KLF6 expression is causally linked to the pathogenesis of periodontitis.[18] On the basis of the findings from bioinformatics analysis and luciferase assays, we first discover that KLF6 is a direct miR-769-5p target. Importantly, our results first highlight KLF6 as a downstream effector of miR-769-5p in controlling LPS-induced hPDLC inflammation and apoptosis.

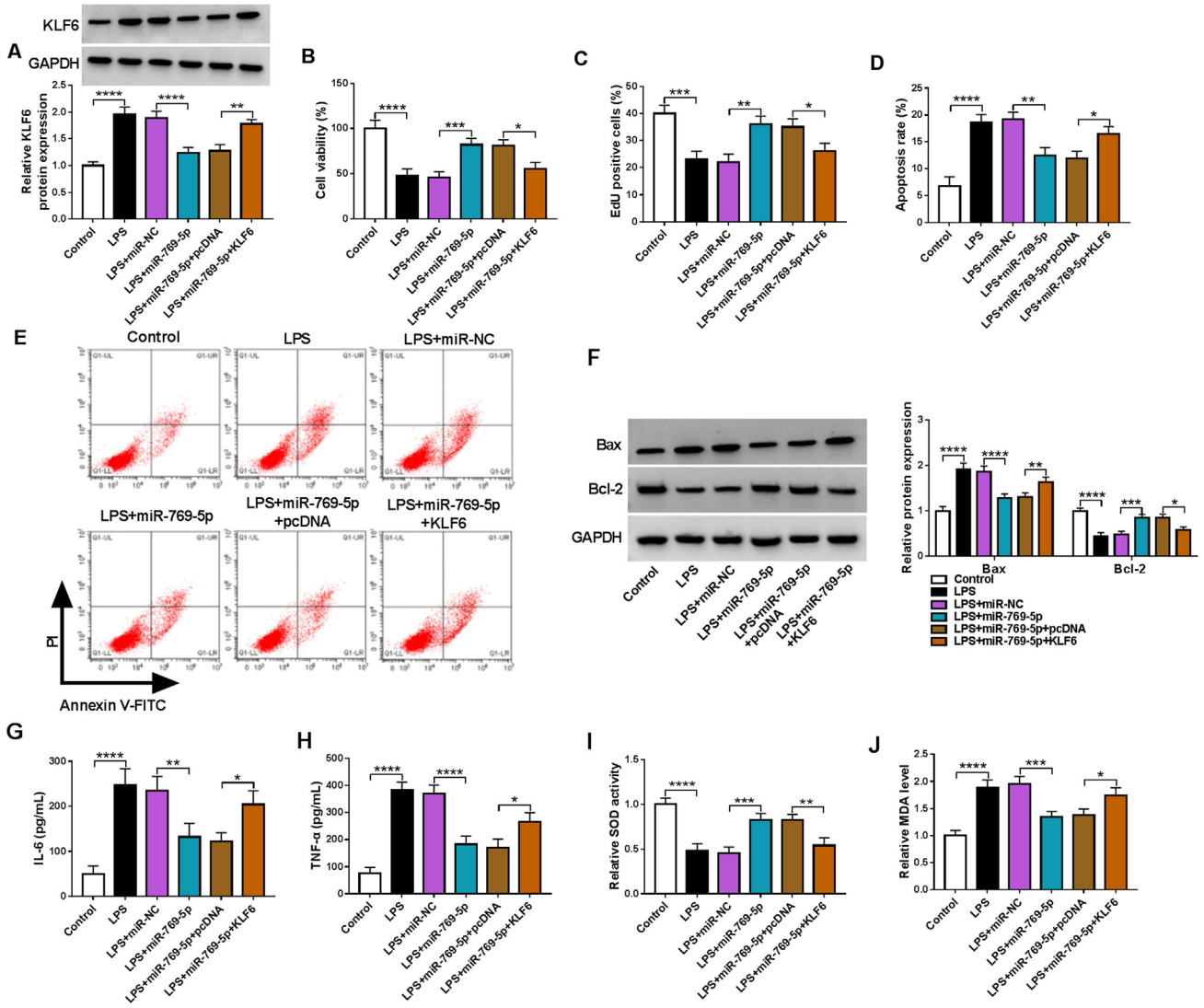

Figure 6 KLF6 is a functional effector of miR-769-5p. (A–J) hPDLCs were transfected with or without miR-769-5p mimic, miR-769-5p mimic + KLF6 expression plasmid, miR-769-5p mimic + pcDNA control or miR-NC mimic before exposure to 0 or 2 μg/mL of LPS for 24 h. (A) Relative KLF6 protein level normalized to GAPDH by Western blot in treated hPDLCs. (B) CCK-8 cell viability assay with hPDLCs after the indicated treatment. (C) EdU cell proliferation assay with hPDLCs after the indicated treatment. (D and E) Assessment of cell apoptosis by flow cytometry based on Annexin V-FITC and PI staining. (F) Western blot of Bax and Bcl-2 expression levels in treated hPDLCs. (G and H) The production levels of IL-6 and TNF-α in treated hPDLCs using ELISA with the assay kits. (I and J) Measurement of SOD activity and MDA level using the assay kits. *$P < 0.05$, **$P < 0.01$, ***$P < 0.001$, ****$P < 0.0001$.

Similarly, miR-543-3p directly targets and inhibits KLF6 to relieve LPS-evoked inflammation and apoptosis in hPDLCs.[18] More interestingly, we prove that circ_0097010 involves post-transcriptional regulation of KLF6 through miR-769-5p, suggesting that the novel circ_0097010/miR-769-5p/KLF6 regulatory axis is involved in LPS-induced cell damage in hPDLCs. Additionally, the expression of circ_0097010/miR-769-5p/KLF6 was closely associated the severity of gingivitis in subjects, suggesting the potential diagnostic value of the novel regulation cascade in gingivitis. Although our findings suggest the implication of the circ_0097010/miR-769-5p/KLF6 axis in hPDLC injury induced by LPS, this study is limited in investigating the role of circ_0097010 in periodontitis pathogenesis due to the lack of *in vivo* analyses using the related animal models.

Of note, KLF6 serves as a co-activator of nuclear factor-kappaB (NF-kappaB) after IL-1β stimulation by interacting with p65 to activate selected downstream genes.[34] Conversely, in glioblastoma cell lines, KLF6 can weaken NF-kappaB nuclear localization and repress NF-kappaB target expression.[35] Since the NF-kappaB signaling is a potent contributor to the inflammatory response in

periodontitis,[36,37] we propose a model in which circ_0097010 might upregulate KLF6 through miR-769-5p to activate the NF-kappaB pathway, leading to periodontitis development. The proposed model will require further investigation.

In summary, these data have identified circ_0097010 as a key regulator of LPS-evoked inflammation and apoptosis in hPDLCs and highlighted a novel mechanism of circ_0097010 regulation through miR-769-5p/KLF6 axis, providing the basis for the development of circRNA-targeted diagnosis, prevention and treatment for periodontitis.

Declaration of competing interest

The authors have no conflicts of interest relevant to this article.

Acknowledgements

None.

Appendix ASupplementary data

Supplementary data to this article can be found online at https://doi.org/10.1016/j.jds.2022.04.024.

References

1. Bartold PM. Lifestyle and periodontitis: the emergence of personalized periodontics. *Periodontol 2000* 2018;78:7—11.
2. Kwon T, Lamster IB, Levin L. Current concepts in the management of periodontitis. *Int Dent J* 2021;71:462—76.
3. Sanz M, Marco Del Castillo A, Jepsen S, et al. Periodontitis and cardiovascular diseases: consensus report. *J Clin Periodontol* 2020;47:268—88.
4. Baeza M, Morales A, Cisterna C, et al. Effect of periodontal treatment in patients with periodontitis and diabetes: systematic review and meta-analysis. *J Appl Oral Sci* 2020;28:e20190248.
5. Kristensen LS, Andersen MS, Stagsted LVW, Ebbesen KK, Hansen TB, Kjems J. The biogenesis, biology and characterization of circular RNAs. *Nat Rev Genet* 2019;20:675—91.
6. Panda AC. Circular RNAs act as miRNA sponges. *Adv Exp Med Biol* 2018;1087:67—79.
7. Han B, Chao J, Yao H. Circular RNA and its mechanisms in disease: from the bench to the clinic. *Pharmacol Ther* 2018;187:31—44.
8. Zhang Y, Wang C, Zhu C, et al. Redondoviridae infection regulates circRNAome in periodontitis. *J Med Virol* 2022;94:2537—47.
9. Jiao K, Walsh LJ, Ivanovski S, Han P. The emerging regulatory role of circular RNAs in periodontal tissues and cells. *Int J Mol Sci* 2021;22.
10. Li W, Zhang Z, Li Y, Wang Z. Abnormal hsa_circ_0003948 expression affects chronic periodontitis development by regulating miR-144-3p/NR2F2/PTEN signaling. *J Periodontal Res* 2021;57:316—23.
11. Wang J, Du C, Xu L. Circ_0081572 inhibits the progression of periodontitis through regulating the miR-378h/RORA axis. *Arch Oral Biol* 2021;124:105053.
12. Wang F, Chen X, Han Y, Xi S, Wu G. circRNA CDR1as regulated the proliferation of human periodontal ligament stem cells under a lipopolysaccharide-induced inflammatory condition. *Mediat Inflamm* 2019;2019:1625381.
13. Li J, Xie R. Circular RNA expression profile in gingival tissues identifies circ_0062491 and circ_0095812 as potential treatment targets. *J Cell Biochem* 2019;120:14867—74.
14. Jin SH, Zhou JG, Guan XY, Bai GH, Liu JG, Chen LW. Development of an miRNA-Array-based diagnostic signature for periodontitis. *Front Genet* 2020;11:577585.
15. Shen Z, Silva RM. MicroRNAs: emerging players in apical periodontitis. *J Appl Oral Sci* 2021;29:e20201058.
16. Chen Q, Cao M, Ge H. Knockdown of MALAT1 inhibits the progression of chronic periodontitis via targeting miR-769-5p/HIF3A axis. *BioMed Res Int* 2021;2021:8899863.
17. Syafruddin SE, Mohtar MA, Wan Mohamad Nazarie WF, Low TY. Two sides of the same coin: the roles of KLF6 in physiology and pathophysiology. *Biomolecules* 2020;10.
18. Li W, Wang J, Hao W, Yu C. MicroRNA-543-3p down-regulates inflammation and inhibits periodontitis through KLF6. *Biosci Rep* 2021;41.
19. Goldsmith CD, Bond DR, Jankowski H, et al. The olive biphenols oleuropein and hydroxytyrosol selectively reduce proliferation, influence the cell cycle, and induce apoptosis in pancreatic cancer cells. *Int J Mol Sci* 2018;19.
20. Iwakawa HO, Tomari Y. The functions of microRNAs: mRNA decay and translational repression. *Trends Cell Biol* 2015;25:651—65.
21. Wang H, Feng C, Wang M, Yang S, Wei F. Circular RNAs: diversity of functions and a regulatory nova in oral medicine: a pilot review. *Cell Transplant* 2019;28:819—30.
22. Du W, Wang L, Liao Z, Wang J. Circ_0085289 alleviates the progression of periodontitis by regulating let-7f-5p/SOCS6 Pathway. *Inflammation* 2021;44:1607—19.
23. Liu H, Hu G, Wang Z, et al. circPTCH1 promotes invasion and metastasis in renal cell carcinoma via regulating miR-485-5p/MMP14 axis. *Theranostics* 2020;10:10791—807.
24. Peng QS, Cheng YN, Zhang WB, Fan H, Mao QH, Xu P. circRNA_0000140 suppresses oral squamous cell carcinoma growth and metastasis by targeting miR-31 to inhibit Hippo signaling pathway. *Cell Death Dis* 2020;11:112.
25. Lee D. miR-769-5p is associated with prostate cancer recurrence and modulates proliferation and apoptosis of cancer cells. *Exp Ther Med* 2021;21:335.
26. Liu W, Wang B, Duan A, et al. Exosomal transfer of miR-769-5p promotes osteosarcoma proliferation and metastasis by targeting DUSP16. *Cancer Cell Int* 2021;21:541.
27. Luan PB, Jia XZ, Yao J. MiR-769-5p functions as an oncogene by down-regulating RYBP expression in gastric cancer. *Eur Rev Med Pharmacol Sci* 2020;24:6699—706.
28. Zhou Y, Xu XM, Feng Y. MiR-769-5p inhibits cancer progression in oral squamous cell carcinoma by directly targeting JAK1/-STAT3 pathway. *Neoplasma* 2020;67:528—36.
29. Sun Y, Li J, Zheng S. MiR-769-5p, which targets HDGF, inhibits cell proliferation and invasion in nonsmall cell lung cancer. *Cancer Biother Radiopharm* 2021. https://doi.org/10.1089/cbr.2021.0363.
30. Cui JY, Liang HW, Pan XL, et al. Characterization of a novel panel of plasma microRNAs that discriminates between Mycobacterium tuberculosis infection and healthy individuals. *PLoS One* 2017;12:e0184113.
31. Kim GD, Ng HP, Patel N, Mahabeleshwar GH. Kruppel-like factor 6 and miR-223 signaling axis regulates macrophage-mediated inflammation. *Faseb J* 2019;33:10902—15.

32. Li D, Liu X, Li C, et al. Role of promoting inflammation of Krüppel-like factor 6 in acute kidney injury. *Ren Fail* 2020;42:693—703.
33. Zhang Y, Li C, Guan C, et al. MiR-181d-5p targets KLF6 to improve ischemia/reperfusion-induced AKI through effects on renal function, apoptosis, and inflammation. *Front Physiol* 2020;11:510.
34. Zhang Y, Lei CQ, Hu YH, et al. Krüppel-like factor 6 is a co-activator of NF-κB that mediates p65-dependent transcription of selected downstream genes. *J Biol Chem* 2014;289:12876—85.
35. Masilamani AP, Ferrarese R, Kling E, et al. KLF6 depletion promotes NF-κB signaling in glioblastoma. *Oncogene* 2017;36:3562—75.
36. Guan X, He Y, Wei Z, et al. Crosstalk between Wnt/β-catenin signaling and NF-κB signaling contributes to apical periodontitis. *Int Immunopharm* 2021;98:107843.
37. Wang J, Wang B, Lv X, Wang L. NIK inhibitor impairs chronic periodontitis via suppressing non-canonical NF-κB and osteoclastogenesis. *Pathog Dis* 2020;78.